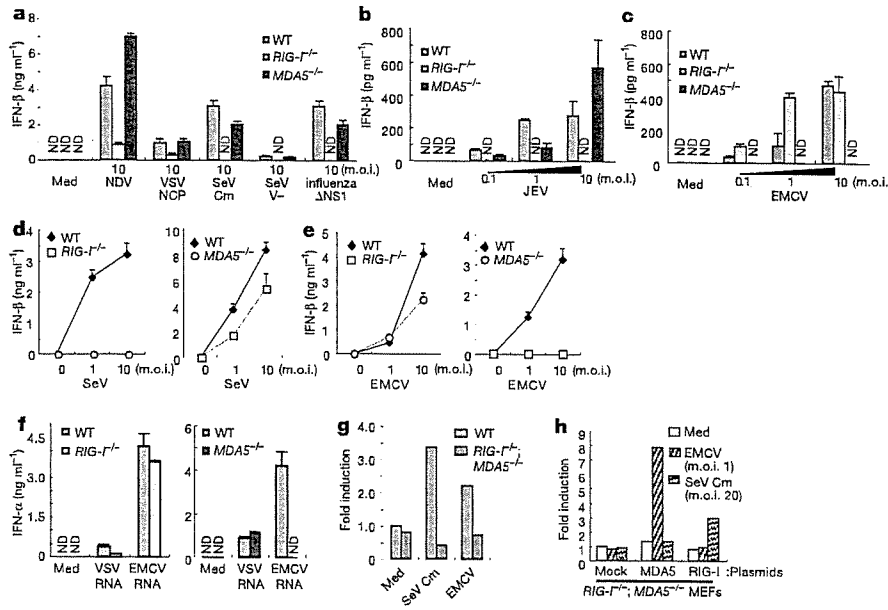

Figure 2 | Differential viral recognition by RIG-I and MDA5. a, Wild-type, *RIG-I*$^{-/-}$ and *MDA5*$^{-/-}$ MEFs were exposed to negative-sense ssRNA viruses, including NDV, VSV lacking a variant of M protein (NCP), SeV with a mutated C protein (Cm), SeV lacking V protein (V^{-}), and influenza virus lacking the NS1 protein (ΔNS1) for 24 h. IFN-β production in the culture supernatants was measured by ELISA. **b**, **c**, Wild-type, *RIG-I*$^{-/-}$ and *MDA5*$^{-/-}$ MEFs were exposed to the positive-sense ssRNA viruses JEV (**b**) and EMCV (**c**), and IFN-β production was measured. **d**, **e**, GMCSF-DCs from *RIG-I*$^{-/-}$ and *MDA5*$^{-/-}$ mice and their littermate wild-type mice were infected with an increasing m.o.i. of SeV V^{-} (**d**) or EMCV (**e**) for 24 h, and IFN-β production was measured. **f**, Wild-type, *RIG-I*$^{-/-}$ and *MDA5*$^{-/-}$ GMCSF-DCs were treated with RNAs directly prepared from VSV and EMCV (complexed with lipofectamine 2000) for 24 h, and IFN-α production was measured. **g**, Wild-type and *RIG-I*$^{-/-}$; *MDA5*$^{-/-}$ MEFs were transiently transfected with a reporter construct containing the *Ifnb* promoter and exposed to SeV Cm or EMCV for 24 h. Cell lysates were then prepared and subjected to a luciferase assay. **h**, RIG-I$^{-/-}$; MDA5$^{-/-}$ MEFs were transiently transfected with the *Ifnb* promoter construct together with expression plasmids encoding human RIG-I or MDA5. The cells were then infected with EMCV or SeV Cm for 24 h and were subjected to a luciferase assay. Error bars in **a**–**g** indicate s.d. of triplicate wells in a single experiment; data are representative of three independent experiments. ND, not detected.

dispensable for the viral induction of IFN-α in pDCs.

We next examined the *in vivo* roles of MDA5 and RIG-I in host defence against viral infection. Although most *RIG-I*$^{-/-}$ mice are embryonic lethal[8], we could efficiently obtain live adult mice by intercrossing the *RIG-I*$^{+/-}$ mice obtained after *RIG-I*$^{+/-}$ × ICR crosses (Supplementary Table 1). When the mice were infected with JEV, serum IFN-α levels were markedly decreased in *RIG-I*$^{-/-}$ mice compared to littermate *RIG-I*$^{+/-}$ mice. In contrast, *MDA5*$^{-/-}$ mice did not show a defect in JEV-induced systemic IFN-α production (Fig. 3a). IFN-α production was partially impaired in *Myd88*$^{-/-}$ mice compared to wild-type mice, but the extent of this impairment was far less than in *RIG-I*$^{-/-}$ mice (Fig. 3a). These data suggest that the TLR system is not critical for the induction of serum IFN-α *in vivo* in response to JEV. Consistent with this finding, *RIG-I*$^{-/-}$ mice, but not *MDA5*$^{-/-}$ or *Myd88*$^{-/-}$ mice, were more susceptible to JEV infection than control mice (Fig. 3b). Furthermore, *RIG-I*$^{-/-}$ mice, but not *MDA5*$^{-/-}$ mice, succumbed to VSV infection, consistent with abrogated interferon responses (Supplementary Fig. 7). Thus, RIG-I-mediated recognition of a specific set of viruses has a critical role in antiviral host defence *in vivo*.

We next challenged the mice with EMCV as a model virus that is recognized by MDA5. Induction of IFN-β, IFN-α, RANTES and IL-6 was severely impaired in the sera of *MDA5*$^{-/-}$ mice (Fig. 4a and Supplementary Fig. 8). *MDA5*$^{-/-}$ mice and mice null for the IFN-α/β receptor (*Ifnar1*$^{-/-}$) were highly susceptible to EMCV infection (viral titre of 1×10^2 plaque-forming units (p.f.u.)) compared to littermate controls ($P < 0.01$) (Fig. 4b). In contrast, deficiency of neither RIG-I nor TLR3 affected the survival of mice infected with EMCV. Consistent with a previous report[22], *Myd88*$^{-/-}$ mice were modestly susceptible to EMCV infection compared to wild-type mice, implying that pDC-mediated responses are not critical for eliminating EMCV (Fig. 4b).

It is known that EMCV preferentially infects cardiomyocytes and causes myocarditis. Consistent with increased susceptibility to EMCV, viral titre in the heart was much higher in *MDA5*$^{-/-}$ mice compared to control mice (Fig. 4c). Histological analysis of hearts two days after EMCV infection revealed that focal necrosis of

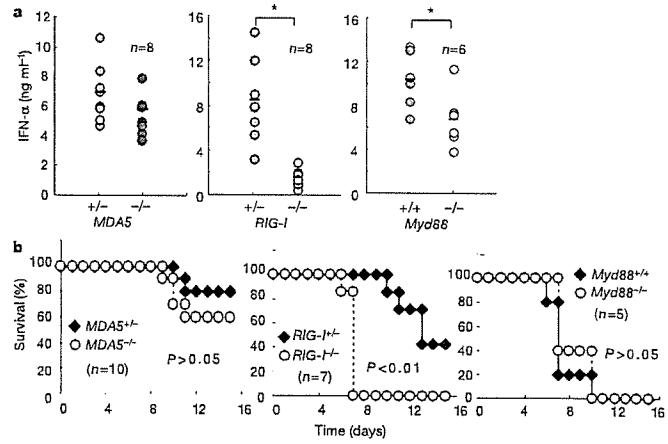

Figure 3 | Susceptibility of *RIG-I*$^{-/-}$ and *MDA5*$^{-/-}$ mice to JEV infection. **a**, *RIG-I*$^{+/-}$, *RIG-I*$^{-/-}$, *MDA5*$^{+/-}$ and *MDA5*$^{-/-}$ mice ($n = 8$), and *Myd88*$^{+/+}$ or *Myd88*$^{-/-}$ mice ($n = 6$), were injected intravenously with 2×10^7 p.f.u. JEV. Sera were collected 24 h after injection, and IFN-α production levels measured by ELISA. Circles represent individual mice, bars indicate mean values. Asterisk, $P < 0.05$ versus controls (*t*-test). **b**, The survival of 6-week-old mice (genotypes as indicated) infected intravenously with 2×10^7 p.f.u. JEV. Mice were monitored for 15 days ($P < 0.01$ between *RIG-I*$^{-/-}$ mice and their littermate controls, generalized Wilcoxon test).

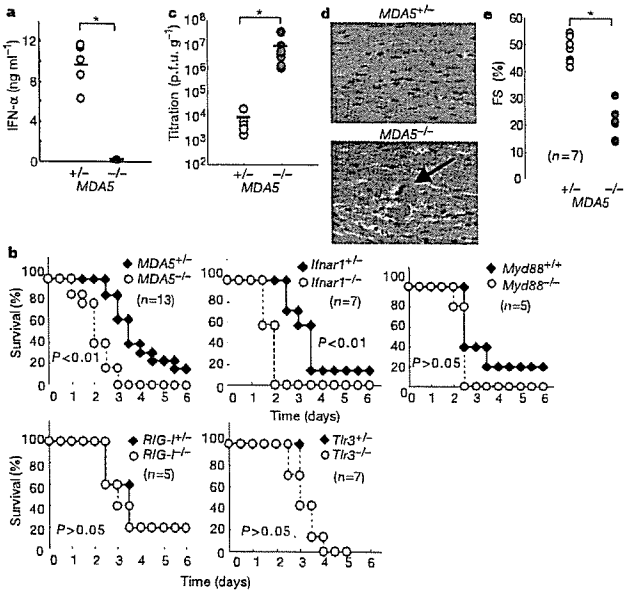

Figure 4 | Role of MDA5 in host defence against EMCV infection. **a**, $MDA5^{+/-}$ and $MDA5^{-/-}$ mice ($n = 5$) were inoculated intravenously with 1×10^7 p.f.u. EMCV. Sera were prepared 4 h after injection and IFN-α production levels determined by ELISA. **b**, The survival of 6-week-old mice (genotypes as indicated) infected with 1×10^2 p.f.u. EMCV intraperitoneally was monitored every 12 h for six days ($P < 0.01$ between $MDA5^{-/-}$ or $Ifnar1^{-/-}$ mice and their littermate controls, generalized Wilcoxon test). **c**, $MDA5^{+/-}$ and $MDA5^{-/-}$ mice were infected intraperitoneally with 1×10^2 p.f.u. EMCV. After 48 h, mice were killed and virus titres in hearts were determined by plaque assay. **d**, Heart sections of $MDA5^{+/-}$ and $MDA5^{-/-}$ mice, two days after infection, were assessed for histological changes using haematoxylin and eosin staining. Arrow indicates the focal necrosis of cardiomyocytes. **e**, Cardiac function of mice 48 h after EMCV infection was assessed by echocardiography (see Supplementary Fig. 8b). The fractional shortening (FS) after infection determined by transthoracic M-mode echocardiographic tracings is shown. Asterisk, $P < 0.05$ versus $MDA5^{+/-}$ mice (*t*-test).

cardiomyocytes had developed in $MDA5^{-/-}$ mice, but wild-type hearts showed no histological abnormalities at this time point (Fig. 4d). Notably, no infiltration of immune cells was observed in either wild-type or $MDA5^{-/-}$ heart sections at this time point. However, when cardiac performance was analysed by echocardiography two days after infection (Fig. 4e), cardiac contractility was severely depressed in $MDA5^{-/-}$ mice (fractional shortening 48.2 ± 4.9% in $MDA5^{+/-}$ mice, 21.2 ± 5.8% in $MDA5^{-/-}$ mice), indicating that $MDA5^{-/-}$ mice developed severe heart failure due to virus-induced cardiomyopathy. Thus, MDA5-mediated recognition of EMCV is a prerequisite for triggering antiviral responses as well as for prevention of myocardial dysfunction.

Together, our results demonstrate that RIG-I and MDA5 have essential roles in the recognition of different groups of RNA viruses, as well as in the subsequent production of type-I interferons and pro-inflammatory cytokines. We have found that poly(I:C) and *in vitro* transcribed dsRNA are recognized by MDA5 and RIG-I, respectively; this is in contrast to results from previous *in vitro* studies. RIG-I probably recognizes dsRNA generated over the course of RNA virus replication, as all *in vitro* transcribed dsRNAs tested except for poly(I:C) induced type-I interferons through RIG-I. In contrast, the endogenous ligand of MDA5 remains enigmatic. Moreover, how RIG-I and MDA5 differentially recognize natural dsRNAs is undetermined. Given that the helicase domains of RIG-I and MDA5 bind to dsRNA, analyses of the crystal structures of these domains should to help achieve a better understanding of the molecular mechanisms underlying this differential recognition. Furthermore, it is still possible that unknown dsRNA-binding proteins also function as direct receptors for viral RNAs.

Finally, the picornavirus family contains several viruses that are pathogenic for humans, including poliovirus, rhinovirus and the virus causing foot-and-mouth-disease. Our studies suggest that human MDA5 and RIG-I also recognize RNA viruses. Thus, identification of therapeutic agents that modify RIG-I or MDA5 may lead to antiviral strategies against selected viruses.

METHODS

Mice, cells and reagents. The generation of $MDA5^{-/-}$ mice is described in the Supplementary Information. $Myd88^{-/-}$, $Tlr3^{-/-}$ and $Trif^{-/-}$ mice have been described previously[12]. $Ifnar1^{-/-}$ mice have also been described previously[25]. $RIG\text{-}I^{+/-}$ mice in a 129Sv × C57BL/6 background were crossed with ICR mice, and the resulting $RIG\text{-}I^{+/-}$ mice were further intercrossed. Interbreeding of these $RIG\text{-}I^{+/-}$ mice produced healthy and fertile $RIG\text{-}I^{-/-}$ offspring, although their number was less than half that of $RIG\text{-}I^{+/+}$ progeny (Supplementary Table 1). $RIG\text{-}I^{-/-}$ and $RIG\text{-}I^{+/-}$ littermate mice were used for *in vivo* experiments. $RIG\text{-}I^{-/-}$; $MDA5^{-/-}$ mice in a 129Sv × C57BL/6 background were lethal at embryonic day 12.5. Additional details regarding cells, reagents and the preparation of *in vitro* transcribed dsRNA are provided in the Supplementary Information.

Viruses. NDV (ref. 3), VSV, VSV lacking a variant of M protein (NCP) (ref. 8), influenza virus lacking the NS1 protein (ΔNS1) (ref. 26), JEV (ref. 27) and EMCV (ref. 3) have been described previously. SeV and SeV lacking the V protein (V^-) or with mutated C proteins (Cm) were provided by A. Kato[28].

Luciferase assay. Wild-type or $RIG\text{-}I^{-/-}$; $MDA5^{-/-}$ MEFs were transiently transfected with a reporter construct containing the *Ifnb* promoter together with an empty vector (mock), or *RIG-I* or *MDA5* expression vectors. As an internal control, a *Renilla* luciferase construct was transfected. Transfected cells were untreated or infected with EMCV or SeV Cm (m.o.i. 20) for 24 h. The cells were lysed and subjected to a luciferase assay using a dual-luciferase reporter assay system (Promega) according to the manufacturer's instructions.

Analysis of mice after EMCV infection. Methods for plaque assays, histological analysis and echocardiography are described in the Supplementary Information.

Measurement of cytokine production. Cell culture supernatants were collected and analysed for IFN-β, IFN-α, IL-6 or IL-12p40 production using enzyme-linked immunosorbent assays (ELISAs). ELISA kits for mouse IFN-α and IFN-β were purchased from PBL Biomedical Laboratories, and those for IL-6, IL-12p40 and RANTES were obtained from R&D Systems.

Statistical analysis. Kaplan–Meier plots were constructed and a generalized Wilcoxon test was used to test for differences in survival between control and mutant mice after viral infection. Statistical significance of any differences in cytokine concentration and ECMV titres was determined using Student's *t*-tests.

Received 30 January; accepted 20 March 2006.
Published online 9 April 2006.

1. Akira, S., Uematsu, S. & Takeuchi, O. Pathogen recognition and innate immunity. *Cell* 124, 783–801 (2006).
2. Katze, M. G., He, Y. & Gale, M. Jr. Viruses and interferon: A fight for supremacy. *Nature Rev. Immunol.* 2, 675–687 (2002).
3. Yoneyama, M. *et al.* The RNA helicase RIG-I has an essential function in double-stranded RNA-induced innate antiviral responses. *Nature Immunol.* 5, 730–737 (2004).
4. Kang, D. C. *et al. mda-5*: An interferon-inducible putative RNA helicase with double-stranded RNA-dependent ATPase activity and melanoma growth-suppressive properties. *Proc. Natl Acad. Sci. USA* 99, 637–642 (2002).
5. Andrejeva, J. *et al.* The V proteins of paramyxoviruses bind the IFN-inducible RNA helicase, mda-5, and inhibit its activation of the *IFN-β* promoter. *Proc. Natl Acad. Sci. USA* 101, 17264–17269 (2004).
6. Yoneyama, M. *et al.* Shared and unique functions of the DExD/H-box helicases RIG-I, MDA5, and LGP2 in antiviral innate immunity. *J. Immunol.* 175, 2851–2858 (2005).
7. Rothenfusser, S. *et al.* The RNA helicase Lgp2 inhibits TLR-independent sensing of viral replication by retinoic acid-inducible gene-I. *J. Immunol.* 175, 5260–5268 (2005).
8. Kato, H. *et al.* Cell type-specific involvement of RIG-I in antiviral response. *Immunity* 23, 19–28 (2005).
9. Iwasaki, A. & Medzhitov, R. Toll-like receptor control of the adaptive immune responses. *Nature Immunol.* 5, 987–995 (2004).
10. Beutler, B. Inferences, questions and possibilities in Toll-like receptor signalling. *Nature* 430, 257–263 (2004).
11. Alexopoulou, L., Holt, A. C., Medzhitov, R. & Flavell, R. A. Recognition of double-stranded RNA and activation of NF-κB by Toll-like receptor 3. *Nature* 413, 732–738 (2001).

12. Yamamoto, M. *et al.* Role of adaptor TRIF in the MyD88-independent toll-like receptor signaling pathway. *Science* **301**, 640–643 (2003).
13. Kovacsovics, M. *et al.* Overexpression of Helicard, a CARD-containing helicase cleaved during apoptosis, accelerates DNA degradation. *Curr. Biol.* **12**, 838–843 (2002).
14. Kawai, T. *et al.* IPS-1, an adaptor triggering RIG-I- and Mda5-mediated type I interferon induction. *Nature Immunol.* **6**, 981–988 (2005).
15. Seth, R. B., Sun, L., Ea, C. K. & Chen, Z. J. Identification and characterization of MAVS, a mitochondrial antiviral signaling protein that activates NF-κB and IRF 3. *Cell* **122**, 669–682 (2005).
16. Xu, L. G. *et al.* VISA is an adapter protein required for virus-triggered IFN-β signaling. *Mol. Cell* **19**, 727–740 (2005).
17. Meylan, E. *et al.* Cardif is an adaptor protein in the RIG-I antiviral pathway and is targeted by hepatitis C virus. *Nature* **437**, 1167–1172 (2005).
18. Fitzgerald, K. A. *et al.* IKKε and TBK1 are essential components of the IRF3 signaling pathway. *Nature Immunol.* **4**, 491–496 (2003).
19. Sharma, S. *et al.* Triggering the interferon antiviral response through an IKK-related pathway. *Science* **300**, 1148–1151 (2003).
20. Hemmi, H. *et al.* The roles of two IκB kinase-related kinases in lipopolysaccharide and double stranded RNA signaling and viral infection. *J. Exp. Med.* **199**, 1641–1650 (2004).
21. Sato, M. *et al.* Distinct and essential roles of transcription factors IRF-3 and IRF-7 in response to viruses for IFN-α/β gene induction. *Immunity* **13**, 539–548 (2000).
22. Honda, K. *et al.* IRF-7 is the master regulator of type-I interferon-dependent immune responses. *Nature* **434**, 772–777 (2005).
23. Chang, T. H., Liao, C. L. & Lin, Y. L. Flavivirus induces interferon-beta gene expression through a pathway involving RIG-I-dependent IRF-3 and PI3K-dependent NF-κB activation. *Microbes Infect.* **8**, 157–171 (2006).
24. Melchjorsen, J. *et al.* Activation of innate defense against a paramyxovirus is mediated by RIG-I and TLR7 and TLR8 in a cell-type-specific manner. *J. Virol.* **79**, 12944–12951 (2005).
25. Hoshino, K., Kaisho, T., Iwabe, T., Takeuchi, O. & Akira, S. Differential involvement of IFN-β in Toll-like receptor-stimulated dendritic cell activation. *Int. Immunol.* **14**, 1225–1231 (2002).
26. Diebold, S. S., Kaisho, T., Hemmi, H., Akira, S. & Reis e Sousa, C. Innate antiviral responses by means of TLR7-mediated recognition of single-stranded RNA. *Science* **303**, 1529–1531 (2004).
27. Mori, Y. *et al.* Nuclear localization of Japanese encephalitis virus core protein enhances viral replication. *J. Virol.* **79**, 3448–3458 (2005).
28. Kato, A. *et al.* Characterization of the amino acid residues of sendai virus C protein that are critically involved in its interferon antagonism and RNA synthesis down-regulation. *J. Virol.* **78**, 7443–7454 (2004).

Supplementary Information is linked to the online version of the paper at www.nature.com/nature.

Acknowledgements We thank all colleagues in our laboratory, K. Takeda, T. Shioda, E. Nakayama and K. Kiyotani for helpful discussions, A. Kato, T. Abe, Y. Mori, B. S. Kim and A. Palmenberg for viruses and plasmids, M. Hashimoto for secretarial assistance, and Y. Fujiwara, M. Shiokawa, N. Kitagaki and A. Shibano for technical assistance. This work was supported by grants from the Ministry of Education, Culture, Sports, Science and Technology in Japan, and from the 21st Century Center of Excellence Program of Japan.

Author Information Reprints and permissions information is available at npg.nature.com/reprintsandpermissions. The authors declare no competing financial interests. Correspondence and requests for materials should be addressed to S.A. (sakira@biken.osaka-u.ac.jp).

Supplementary Information

I. Supplementary Materials and Methods

II. Supplemental Figure Legends

III. Supplemental Figures

I. Supplementary Materials and Methods

Generation of MDA5$^{-/-}$ mice

The MDA5 gene was isolated from genomic DNA extracted from ES cells (GSI-I) by PCR. The targeting vector was constructed by replacing a 4.3-kb fragment encoding the MDA5 ORF (including DExH box) with a neomycin-resistance gene cassette (*neo*), and a herpes simplex virus thymidine kinase (HSV-TK) driven by PGK promoter was inserted into the genomic fragment for negative selection. After the targeting vector was transfected into ES cells, G418 and gancyclovir doubly resistant colonies were selected and screened by PCR and further confirmed by Southern blotting. Homologous recombinants were micro-injected into C57BL/6 female mice, and heterozygous F1 progenies were intercrossed in order to obtain MDA5$^{-/-}$ mice. MDA5$^{-/-}$ and littermate control mice were used throughout the experiments.

Cells and Reagents

RIG-I$^{-/-}$ or MDA5$^{-/-}$ MEFs were prepared from embryos under 129Sv and C57BL/6 background derived at 12.5 days postcoitum. RIG-I$^{-/-}$MDA5$^{-/-}$ MEFs were prepared from embryos (129Sv X C57BL/6 background) at 11.5 days postcoitum. Bone marrow derived DCs were generated in RPMI 1640 medium containing 10% FCS, 50 mM 2-mercaptoethanol, and 10 ng/ml GM-CSF or 10 ng/ml Flt3L. pDCs and cDCs were isolated from Flt3L-DCs by MACS using anti-B220 and CD11c microbeads from

Miltenyi Biotech as described. Poly I:C was purchased from Amersham Biosciences. For the synthesis of poly I:C, poly I (152-539 bases) and poly C (319-1305 bases) have been separately synthesized and then annealed. Therefore, the expected length of poly I:C is 319-539 bps (Amersham Bisciences). Poly I:C was complexed with cationic lipids, Lipofectamin 2000 reagents (Invitrogen), and added to MEFs. DCs were incubated with or without Lipofectamine 2000 for stimulation.

Northern blot

PECs were treated with or without 1000 U/ml mouse IFN-β (Calbiochem) for 8 h, and total RNA was extracted using TRIzol reagent (Invitrogen). RNA was electrophoresed, transferred to nylon membranes and then hybridized with indicated cDNA probes. To detect the expression of MDA5 mRNA, a 308 bp fragment (777-1084) was used as a probe. The same membrane was rehybridized with a β-actin probe.

Western blot analysis and an antibody

MEF were treated with 1000 U/ml IFN-β for 8 h. Cells were then lysed in a lysis buffer containing 1.0% Nonidet-P40, 150 mM NaCl, 20 mM Tris-Cl (pH7.5), 1 mM EDTA and protease inhibitor cocktail (Roche). Cell lysates were dissolved by SDS-PAGE and transferred onto a PVDF membrane. The membrane was blotted with the specific antibody to MDA5 protein, and visualized with an enhanced chemiluminescence system (Perkinermer). Polyclonal anti-MDA5 antibody was raised against corresponding to amino acids 1005-1019 of mouse MDA5.

Preparation of in vitro transcribed dsRNA

The mouse Lamin A/C cDNA sequence was amplified by PCR and cloned into the pT7 blue T vector (Novagen) and sequenced. Various lengths of dsRNAs corresponding to the sequence of mouse Lamin A/C were generated using a T7 RiboMAX^{TM} Express RNAi

System (Promega) according to the manufacturer's instruction. In brief, DNA fragments tagged with T7 RNA polymerase promoters corresponding to parts of Lamin A/C (50, 100, 200, 400, 600, 1000 bps) were amplified by a PCR reaction using Lamin A/C cDNA as a template, and with following primers;

T7 Lamin. Forward, TAATACGACTCACTATAGGacttgttggctgcgcaggc

T7 Lamin.50 reverse, TAATACGACTCACTATAGGtgagaagagcctcgaggtcctt

T7 Lamin.100 reverse, TAATACGACTCACTATAGGcaatgtgcgcttctcactgagagcag

T7 Lamin.200 reverse, TAATACGACTCACTATAGGccactcgcctcagcatctcat

T7 Lamin.400 reverse, TAATACGACTCACTATAGGctgttccacctggtcctcatg

T7 Lamin.600 reverse, TAATACGACTCACTATAGGtcctccaggtcacgcagcttt

T7 Lamin.1000 reverse, TAATACGACTCACTATAGGggacttgttgcgcagccgcacgaac

The PCR products were purified and used as templates for in vitro transcription with T7 RNA polymerase. The product was annealed to form dsRNA followed by treatment with DNase and RNase to digest ssRNA and DNA. The dsRNA was further purified by isopropanol precipitation and resuspended in Nucrease-free water. The generation of dsRNAs was visualized by Agarose gel electrophoresis (Supplementary Fig. 2b). To stimulate MEFs, the dsRNA was complexed with Lipofectamine 2000, then added to the cells, and incubated for 24 hours.

Histological analysis

Hearts were taken from EMCV infected mice, and fixed with 3.7% formaldehyde. Transverse sections through the heart (5 μm) were cut and stained with hematoxylin and eosin.

Plaque assay

Forty-eight hours after EMCV infection, Hearts were prepared and homogenized in PBS. Virus titration in the virus containing PBS was determined by standard plaque assay as

described previously[8]. After centrifugation, supernatants were serially diluted, and added to plates containing HeLa cells. The cells were overlaid with DMEM containing 1% low melting agarose and incubated for 48 h. Then plaques were counted.

Echocardiography

Two days after EMCV infection, echocardiography was performed on mice anesthetized with 2.5% avertin (8 μl/g) using ultra-sonography (SONOS-5500, equipped with a 15-MHz linear transducer, Philips Medical Systems). Hearts were imaged in a two-dimensional parasternal short-axis view, and an M-mode echocardiogram of the midventricle was recorded at the level of the papillary muscles*. Heart rate, anterior and posterior wall thickness, and end-diastolic and end-systolic internal dimensions of the LV were obtained from the M-mode image.

Viruses

Mengo virus[1] was kindly provided by A. Palmenberg. Theiler's virus[2] have been described previously.

Preparation of viral RNA.

BHK cells and L cell plated on 10 X 15 cm dishes were infected with moi= 0.01 of wt VSV and EMCV, respectively. At 1h after infection, medium was removed and replaced with DMEM containing 10 % FCS and the cells were incubated for 2 days at 37 °C. Then the supernatants were collected and centrifuged at 3,000 rpm for 15 min to remove cells for avoiding cellar RNA contamination. Then the supernatants were harvested and centrifuged at 25,000 rpm for 90 min in an SW28 rotor at 4 °C. The viral pellet was suspended in TRIzol reagent (Invitrogen) and RNA was extracted. 5-10 μg/ml VSV RNA and 0.5-3 μg/ml EMCV RNA were obtained from single preparation.

Analysis of total protein synthesis.

Cultures of wild-type and MDA5$^{-/-}$ MEFs were infected with EMCV. At various time of labeled by incorporation of 50 μCi of [^{35}S]Met-Cys (GE Healthcare) for 1 h. Then the cells were lysed in a lysis buffer containing 1.0% Nonidet-P40, 150 mM NaCl, 20 mM Tris-Cl (pH7.5), 1 mM EDTA and protease inhibitor cocktail (Roche). Total cell extracts were separated by polyacrylamide gel electrophoresis, and the proteins were visualized by autoradiography.

1. Martin, L. R., Neal, Z. C., McBride, M. S. & Palmenberg, A. C. Mengovirus and encephalomyocarditis virus poly(C) tract lengths can affect virus growth in murine cell culture. J Virol 74, 3074-81 (2000).
2. Shin, T. & Koh, C. S. Immunohistochemical detection of osteopontin in the spinal cords of mice with Theiler's murine encephalomyelitis virus-induced demyelinating disease. Neurosci Lett 356, 72-4 (2004).

II. Supplemental Figure Legends

Supplementary Fig. 1: Targeted disruption of the murine MDA5 gene.

(a) Structure of the mouse *MDA5* gene, the targeting vector and the predicted disrupted gene. Closed boxes denote the coding exon. B; BamH I (b) Southern blot analysis of offspring from the heterozygote intercrosses. Genomic DNA was extracted from mouse tails, digested with BamHI, separated by electrophoresis and hybridized with the radiolabelled probe indicated in (a). Southern blot gave a single 9.4 kb band for wild-type (+/+), a 4.6 kb band for homozygous (-/-) and both bands for heterozygous (+/-) mice. (c) Nothern blot analysis of peritoneal exudates cells (PECs). Total RNA from wild-type (WT) and MDA5$^{-/-}$ PECs treated with 1000 U/ml IFN-β for 8 h was extracted and subjected to Northern blot analysis for the expression of *MDA5* mRNA. The same

membrane was rehybridized with a *β-actin* probe. (d) Western blot analysis of MDA5 expression. WT and MDA5$^{-/-}$ MEFs were treated with 1000 U/ml IFN-β for 8 h, and whole cell lysates were immunoblotted with antibody against MDA5. N.S. non specific.

Supplementary Fig. 2. Involvement of MDA5 or RIG-I in the recognition of dsRNAs.

(a) RIG-I$^{-/-}$ and MDA5$^{-/-}$, and their littermate WT mice were injected intravenously with 200 μg of poly I:C for the indicated periods and the production of IFN-β in the sera was measured by ELISA. The data are means ± S.D. of sera samples.

(b) GMCSF-DCs from RIG-I$^{-/-}$ and MDA5$^{-/-}$, TRIF$^{-/-}$ and their littermate control mice were incubated in the presence of 50, 250 μg/ml poly I:C for 24 h. The production of IFN-α in the culture supernatants was measured by ELISA.

(c) Generation of different lengths of dsRNAs corresponding to mouse lamin A/C. Different lengths of dsRNAs corresponding to mouse lamin A/C were synthesized as described in Methods section. 1 μg of dsRNAs were separated on 1% Agarose gel and visualized by staining with ethidium bromide. All dsRNAs synthesized appear with the estimated size.

Supplementary Fig. 3: Contribution of RIG-I and MDA5 in the induction of genes encoding type I IFNs and IFN-inducible proteins in response to viral infection.

(a) WT, RIG-I$^{-/-}$ or MDA5$^{-/-}$ MEFs were treated with 5 μg/ml poly I:C complexed with lipofectamine 2000 for the indicated periods. Total RNA was extracted and subjected to the Northern blot analysis for the expression of *IFN-β*, *IP10* and *β-actin* mRNA.

(b) WT, RIG-I$^{-/-}$ and MDA5$^{-/-}$ MEFs were treated with 5 μg/ml dsRNA corresponding to Lamin A/C (600 bps) complexed with lipofectamine 2000 for the indicated periods. Total RNA was extracted and subjected to the Northern blot analysis for the expression of

IFN-β and *IP10* mRNA. 28S and 18S ribosomal RNA bands on ethidium bromide-stained gel were used to control the RNA loading (lower panel).

(c) WT, RIG-I$^{-/-}$ and MDA5$^{-/-}$ MEFs were infected with moi=10 of SeV V(-) for the indicated periods. Total RNA was extracted and subjected to the Northern blot analysis for the expression of *IFN-β* and *IP10* mRNA. 28S and 18S ribosomal RNA bands on ethidium bromide-stained gel were used to control the RNA loading (lower panel).

(d) WT and MDA5$^{-/-}$ PECs were exposed to moi=10 of EMCV for the indicated periods. Total RNA was extracted and subjected to the Northern blot analysis for the expression of *IFN-β, IP10, IL-6* and *β-actin* mRNA.

Supplementary Fig. 4: Role of MDA5 and RIG-I in the IFN-α responses against various viruses.

(a) WT, RIG-I$^{-/-}$ and MDA5$^{-/-}$ MEFs were exposed to negative-sense ssRNA viruses, including NDV, VSV NCP, SeV Cm, SeV V- and influenza ΔNS1. IFN-α production in the culture supernatants was measured by ELISA.

(b and c) GMCSF-DCs from RIG-I$^{-/-}$ and MDA5$^{-/-}$ mice and their littermate WT mice were infected with indicated moi of EMCV for 24 h. The production of IFN-α (b) and IL-6 (c) in the culture supernatants was measured by ELISA.

(d) GMCSF-DCs from wild-type and MDA5$^{-/-}$ mice were infected with indicated moi of Theiler's virus or Mengovirus for 24 h. IFN-α production in the culture supernatants was measured by ELISA. The data are means ± S.D. of tripricates.

Supplementary Fig. 5: EMCV-mediated protein synthesis shutoff was not altered between wild-type and MDA5$^{-/-}$ MEFs.

Cultures of wild-type and MDA5$^{-/-}$ MEFs were infected with EMCV and labeled by incorporation of [^{35}S]Met-Cys for 1 h at various times after infection. Total cell extracts

were separated by polyacrylamide gel electrophoresis, and the proteins were visualized by autoradiography.

Supplementary Fig. 6: Differential involvement of MDA5 and MyD88 in EMCV-mediated IFN production in cDCs and pDCs.

DCs were induced from bone marrow cells obtained from $MyD88^{+/-}$, $MyD88^{-/-}$, $MDA5^{+/-}$ and $MDA5^{-/-}$ mice by cultivating in the presence of Flt3L. At day 7, $B220^{+}CD11c^{+}$ pDCs and $B220^{-}CD11c^{+}$ cDCs were purified by MACS, and infected with EMCV for 24h. IFN-α production in the culture supernatants was measured by ELISA. Error bars indicate ± S.D. of triplicates.

Supplementary Fig. 7: The survival of $MDA5^{-/-}$, $RIG\text{-}I^{-/-}$ or $IFN\alpha/\beta R^{-/-}$ mice in response to VSV infection.

The survival of the mice (3-weeks old) infected with $4x10^{6}$ pfu VSV intranasally was monitored for 9 days ($p<0.01$ by the generalized wilcoxon test between $RIG\text{-}I^{-/-}$ mice and their littermate controls).

Supplementary Fig. 8: Responses of $MDA5^{-/-}$ mice against EMCV infection

(a) $MDA5^{+/-}$ and $MDA5^{-/-}$ mice (n=5) were intravenously inoculated with 1 X 10^{7} pfu EMCV. Sera were taken at 4 h after injection, and IFN-β, Rantes and IL-6 production levels were determined by ELISA. *, $P<0.05$ versus controls by the student's t-test.

(b) Cardiac function of the mice 48 h after EMCV infection was assessed by echocardiography. Transthoracic M-mode echocardiographic tracings from $MDA5^{+/-}$ and $MDA5^{-/-}$ mice 48 h after EMCV infection.

Supplementary Table I: Genotypes of mice derived from $RIG\text{-}I^{+/-}$ intercrosses or crosses between $RIG\text{-}I^{+/-}$ and $RIG\text{-}I^{-/-}$ mice.

mental Figure 1.

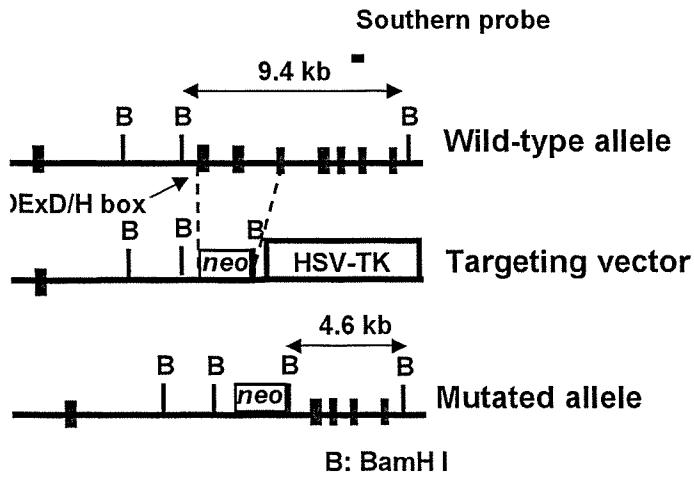

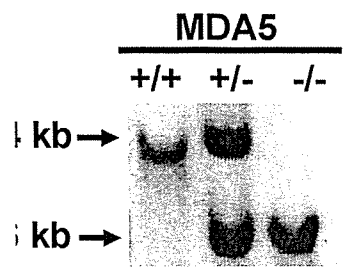

c

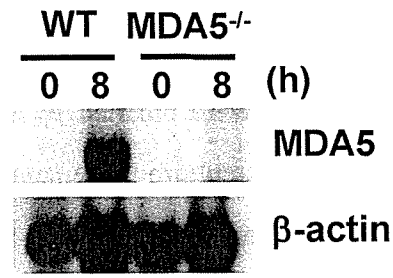

d

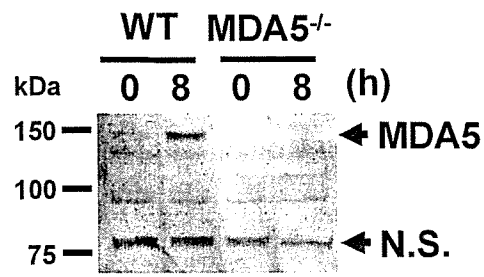

mental Figure 2.

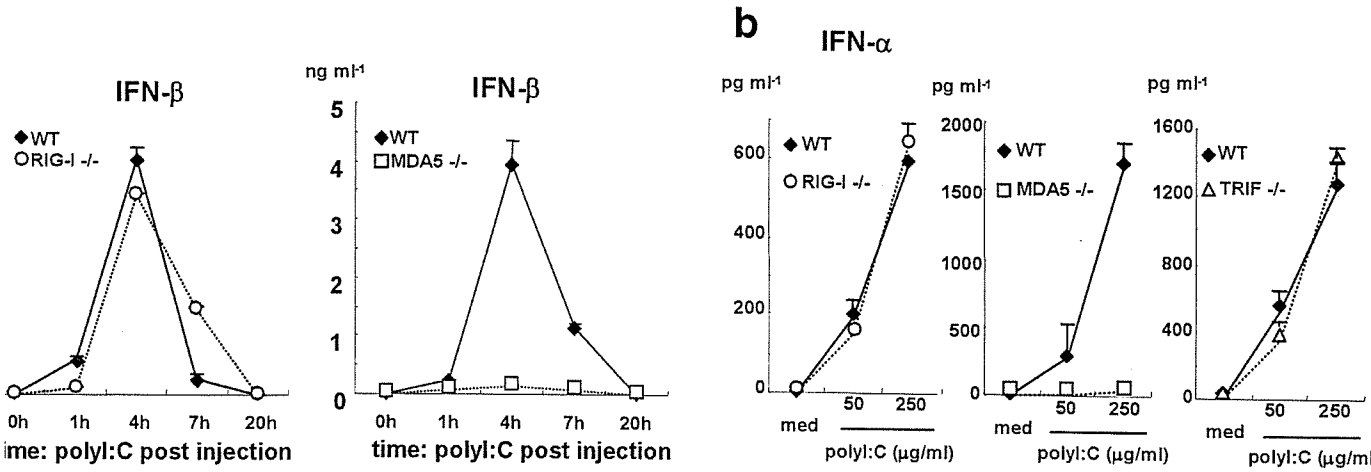

vitro transcribed dsRNA

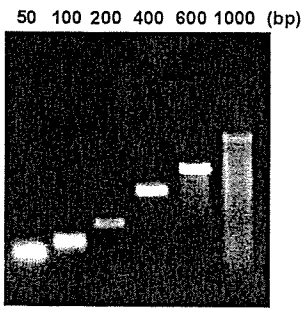

mental Figure 3.

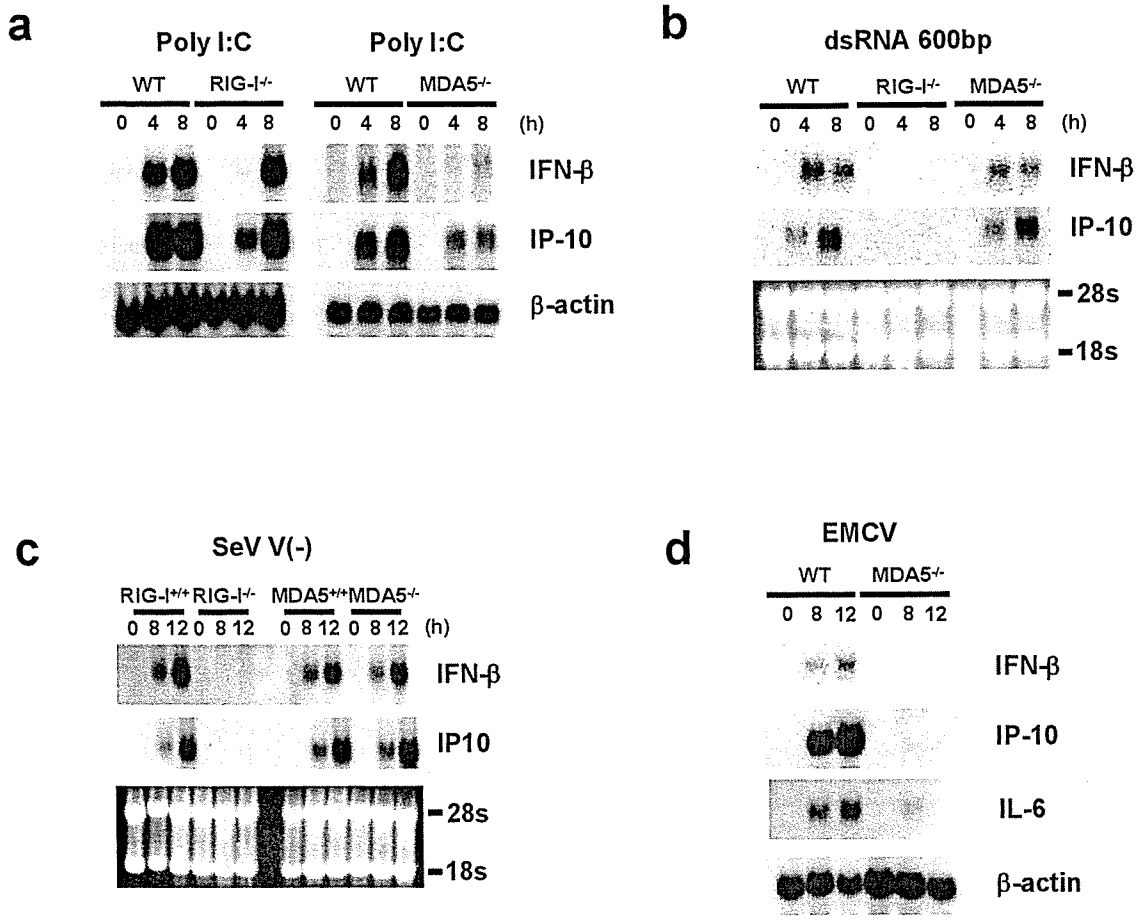

mental Figure 4.

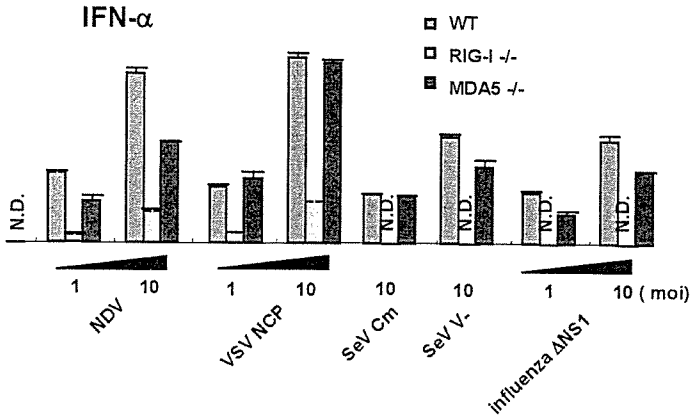

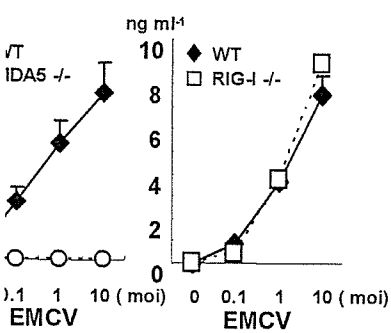

c

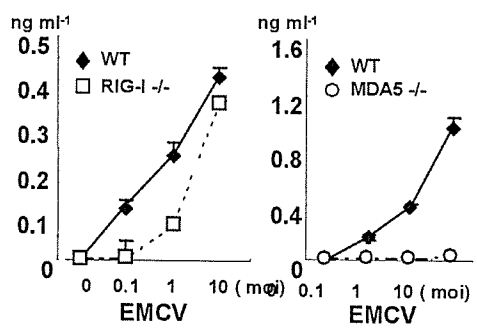

d

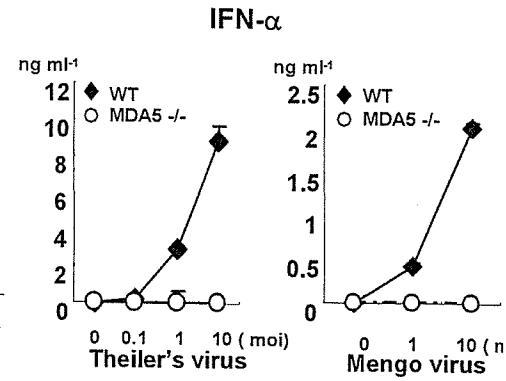

mental Figure 5.

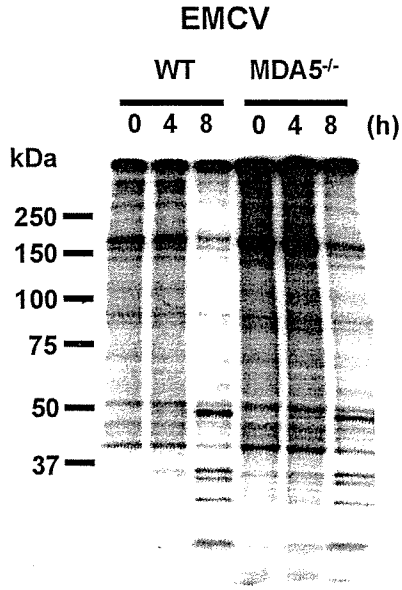

mental Figure 6.

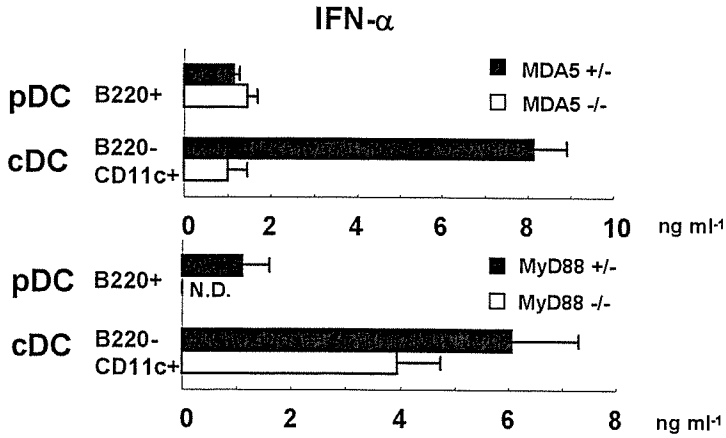

mental Figure 7.

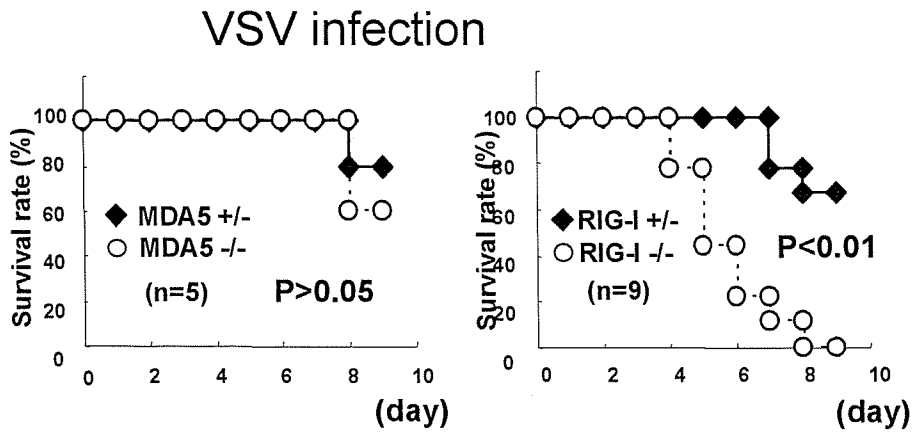

mental Figure 8.

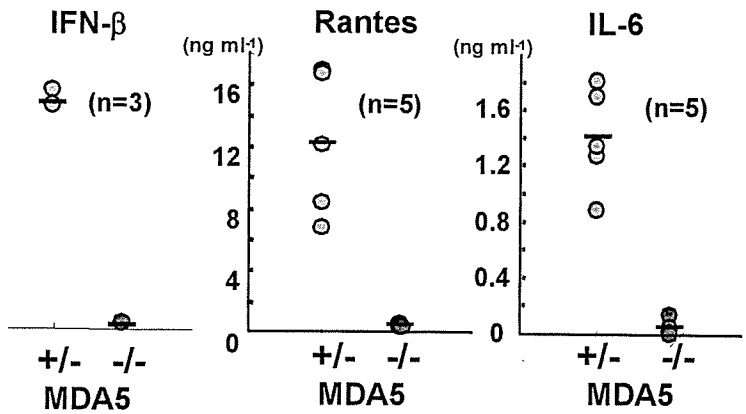

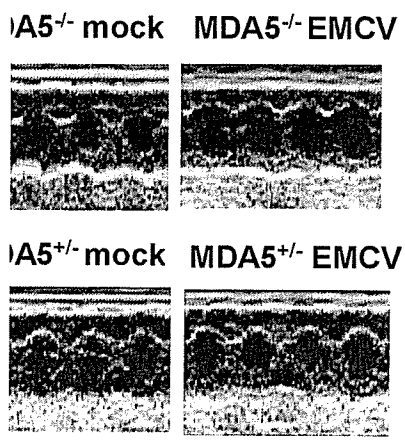

mental Table 1.

a

	RIG-I$^{+/+}$	RIG-I$^{+/-}$	RIG-I$^{-/-}$	Total (%)
Postnatal (6w~)	16 (34)	28 (60)	3 (6)	47 (100)

b

	RIG-I$^{+/-}$	RIG-I$^{-/-}$	Total (%)
Postnatal (6w~)	108 (83)	22 (17)	130 (100)